EEET ECOLOGICAL ENGINEERING & ENVIRONMENTAL TECHNOLOGY

Ecological Engineering & Environmental Technology, 2025, 26(3), 301–314
https://doi.org/10.12912/27197050/200074
ISSN 2719–7050, License CC-BY 4.0

Received: 2024.12.21
Accepted: 2025.01.24
Published: 2025.02.01

Evaluation of land use and land cover changes on groundwater resources in the Pasi Watershed, Pasi Gusung Island, Selayar Islands

Fachrie Musdalipah[1*], Zubair Hazairin[2], Akil Arifuddin[3], Thamrin Putri Saridayana[4]

[1] Regional Planning and Development Study Program, Hasanuddin University, 90245, Makassar, Indonesia
[2] Urban Planning and Design, Department of Urban and Regional Planning, Hasanuddin University, 90245, Makassar, Indonesia
[3] Department of Soil Science, Faculty of Agriculture, Hasanuddin University, 90245, Makassar, Indonesia
[4] Forestry Science Study Program, Faculty of Forestry, Hasanuddin University, 90245, Makassar, Indonesia
* Corresponding author's e-mail: musdalipah23p@student.unhas.ac.id

ABSTRACT

Water is of vital importance to ecosystems and human societies. Because of this, the UN Secretary-General has included the availability of clean water as one of the sustainable development goals (SDGs). This study examined the impact of land use and land cover (LULC) changes on groundwater availability in the Pasi watershed on Pasi Gusung Island, Selayar Islands. LULC changes significantly influence water balance as they determine infiltration and surface runoff patterns. Using cellular automata (CA) integrated with artificial neural network (ANN) modeling via the MOLUSCE plugin in QGIS, historical LULC data from 2014 to 2023 were examined and changes through 2033 were forecasted. The soil and water assessment tool (SWAT) was utilized to evaluate the impact of these changes on water availability. The analysis revealed significant LULC alterations, including the expansion of residential and agricultural areas, a decline in mangrove forests, and reduced groundwater recharge capacity. SWAT results suggest a potential reduction in groundwater storage due to decreased infiltration linked to LULC transformations. This study shows a close relationship between land use and land cover changes and fluctuations in groundwater availability in the Pasi watershed. Analysis of land cover from 2014 to 2023 and projections to 2033 show patterns of change that affect the hydrology of the area, including groundwater discharge and the balance between water availability and demand. Continued population growth pressures already limited water resources, creating a growing annual water deficit. This research provides strategic insights for developing sustainable water supply systems in response to projected land use change.

Keywords: land use land cover, land cover change, cellular automata, MOLUSCE, soil and water assessment tool, groundwater availability.

INTRODUCTION

Water is of vital and critical importance to ecosystems and human societies (Liu et al., 2023). The effects of human activities on land and water are now extensive. These reflect physical changes to the environment. Global changes such as urbanization, population growth, socioeconomic change, evolving energy needs, and climate change have exerted unprecedented pressure on water resources systems. It is argued that achieving global water security is the key to sustainable development (Diansyukma, 2021; Mishra et al., 2021). International concern about the security of the global water supply has grown over the past two to three decades, and there is a need for a more comprehensive strategy to produce sustainable solutions that meet the escalating problems with water management (Falconer, 2022). Access to safe water sources and sanitation for everyone is one of the sustainable development goals (SDGs), which the United Nations (UN) has declared a human right. About 70% of the Earth's surface is covered in water, with about 97.5% of that water being salty or seawater. The sad thing is that only about 2.5% of this freshwater is

usable by humans, with the remainder still existing in the form of frozen water from glaciers and underground water (Hotloś, 2008).

The amount of water in an area on the Earth's surface will always be the same from time to time. The only difference is the hydrological process that takes place in that area. The hydrological cycle is when water moves from the atmosphere to the earth and back again. This cycle is vital in the relationship between groundwater and surface water. LULC can affect the watershed's water balance by affecting the amount of surface runoff, interflow, base flow, and evapotranspiration (Sulamo et al., 2021). If LULC has many elements that make the water that falls to the ground more absorbed into the soil, there will be more water in the soil basin. However, if in the process LULC has less media to absorb water, then the water will become surface water or water flowing on the ground (Pan et al., 2018).

Land cover change refers to permanent land characteristics, such as vegetation type and soil condition. Land cover change is a term used to describe permanent land characteristics, such as vegetation type and soil condition. Meanwhile, LULC change refers to the changes in the way humans utilize or manage a piece of land under a planning concept (Nedd et al., 2021). Increased agriculture, urbanization, deforestation, and human activity all contribute to changes in LULC throughout time and space, while changes in land cover affect the pattern of water availability and water balance (Jamal and Ahmad, 2020).

The Pasi watershed is crucial in supporting the ecosystem and life on Pasi Gusung Island. The water that flows through this watershed supports agriculture and fisheries and is a significant source of drinking water supply. However, challenges include limited access to clean water, fluctuations in water quality, as well as the threat of pollution and climate change that can affect water availability. This study aimed to bridge the gap in understanding the relationship between land cover change and groundwater availability. In previous studies, LULC affected water supply at the watershed scale. These systemic changes will have compounding effects on water availability (Martin, 2021). This study hypothesized that land cover change significantly affects groundwater discharge, with additional contributions from climatic factors, population growth, and human activities leading to increased water deficits yearly. LULC changes were captured and predicted using CA analysis using an ANN on the Molusce plugin in QGIS. Water availability and balance are evaluated using the QSWAT feature in the QGIS application. The land cover used as the present is the land cover in 2023, and the land cover used as a future prediction is the land cover prediction in 2033. This comprehensive approach provides a more holistic and strategic overview for developing and sustaining community-based water supply systems.

MATERIALS AND METHODS

Pasi Gusung Island is a small island located within the Pasi watershed. Pasi Gusung Island is an island in the Bontoharu sub-district of Selayar Islands Regency with an area of approximately 2.306 hectares. Pasi Gusung Island is administratively located in Bontoharu Sub-district and consists of 3 villages: Bontoborusu Village, Kahu-Kahu Village and Bontolebang Village (Table 1). Geographically, Pasi Gusung Island is located at 120°23'32.03"–120°25'59.87" East Longitude and 6°6'18.46"–6°12'32.52" South latitude (Government of Selayar Islands Regency, 2023). The island's geographical location within the Pasi watershed provides unique challenges and opportunities for water resources management, particularly in providing adequate water to the local population (Figure 1).

Cellular automata (CA) analysis using artificial neural network (ANN)

Before looking at current and future water availability, the authors first considered land cover and land use on Pasi Gusung Island in 2023 and predicted LULC for 2033. LULC change detection

Table 1. Territory and area of Pasi Gusung Island

District	Sub-district/Village	Area (Ha)	Percentage (%)
Bontoharu	Bontoborusu	1245.68	54.02
	Bontolebang	451.74	19.59
	Kahu-Kahu	608.59	26.39
Total		2306.01	100.00

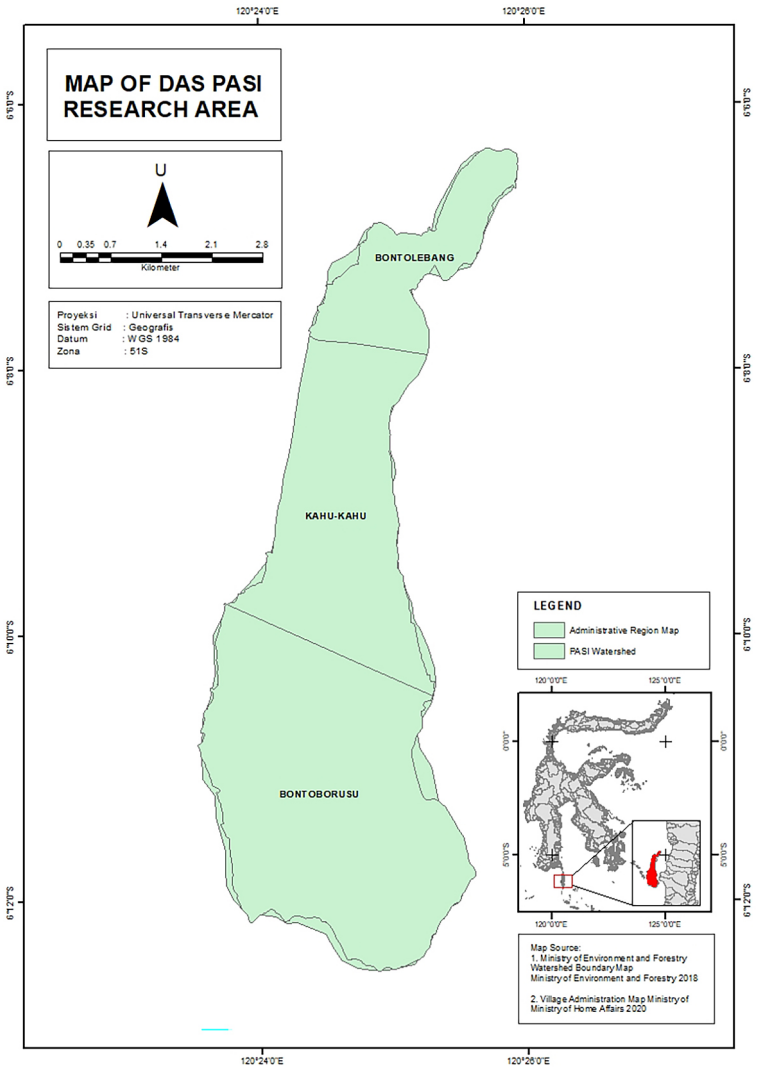

Figure 1. Map of the Pasi Gusung Island research site within the PASI watershed catchment area

and forecasting are essential factors to guide planning, land resources, and sustainable development management (Degerli and Çetin, 2022). The land cover prediction simulation model is an effective and repeatable technique to evaluate the causes and impacts of past, present and future scenarios in various situations (Abbas et al., 2021). For the projection of land cover, the CA analysis method with ANN is used, which uses the Modules for LULC Change Evaluation (MOLUSCE) plugin from the QGIS application (Indhanu et al., 2025; Setiawan and Nandini, 2022).

The stages and data requirements for the CA analysis method with ANN using the MOLUSCE plugin from the QGIS application are as follows:

Land cover data: land cover data for 2014, 2019, and 2023 taken from Landsat 8–9 OLI/TIRS C2 L2 (Dibs et al., 2023) were obtained from the USGS Earth Explorer website (https://earthexplorer.usgs.gov/) imagery using bands 6,5,4 to view land cover with false color or false combination bands used to display objects with spectra invisible to the human eye. With these various band combinations, it is possible to analyze satellite images for multiple purposes such as land, vegetation, water, or urbanization analysis. One commonly used combination is the combination for analyzing vegetation and landscapes. Historical data is a reasonable basis for prediction, but the more land cover data from the past, the more accurate the prediction can be. Consistent land cover data from multiple time points is required to train the prediction model.

Driving factors: in the MOLUSCE plugin, there are so-called driving factors, which are variables or factors that influence and drive land cover change over time. These factors are used to model and predict future LULC change by

accounting for environmental, social, and economic influences on land cover dynamics. The driving factors consist of three categories: natural factors, built-up land factors, and socio-economic factors (Kim and Newman, 2020). The following Table 2 shows the variables of each class.

This study used data on population density per ha as the driving factor. This factor measures the influence of population on land change. The areas with high population density usually experience faster change, for example into residential areas (Table 3).

The method used in the MOLUSCE plugin with ANN: MOLUSCE calculates land change from time A to time B by comparing two LULC maps from different periods. This data is analyzed to find the relationship between driving factors and land change (Degerli and Çetin, 2022). Validation of the MLP-ANN model is critical. Therefore, validation between the QGIS MOLUSCE extension and the Cellular Automata model resulted in kappa coefficients. The kappa coefficient (or Kappa statistic, often called Cohen's Kappa) is a statistical measure used to assess the degree of agreement or consistency between two observers or models, considering the possibility of agreement occurring by chance. It is often used in spatial classifications (such as land use maps) or reliability testing in categorical data studies (Tong and Feng, 2020).

The general scale of kappa interpretation:

- 0.81–1.00 : excellent category,
- 0.61–0.80 : good category,
- 0.41–0.60 : medium category,
- 0.21–0.40 : weak category,
- 0.01–0.20 : very weak category,
- ≤ 0 : no category or worse than random.

In the context of LULC change modeling (such as MOLUSCE), the kappa coefficient is used to evaluate how well the predictive model (e.g., cellular automata) matches the actual observational data, giving an idea of the accuracy of the simulation results to reality.

After projecting the land cover for the next 10 years to 2033 using CA analysis with ANN, a SWAT model analysis can be carried out for the 2023 land cover and 2033 land cover predictions. In addition, the projected population of Pasi Gusung Island for the next 10 years was obtained from the average population growth data published by the Central Statistics Agency of Bontoharu District, Selayar Islands Regency. This method is used to compare water availability in 2033 and the population in that year, whether it is still sufficient or insufficient.

Table 2. Classification of driving factors for land cover projection with the MOLUSCE plugin in QGIS

Classification	Driving factors
Natural factors	Slope
	Distance to river
Buildable land factor	Distance to road
	Residential
Socio-economic factors	Population density

SWAT model analysis

The soil and water assessment tool (SWAT) model was first developed by the United States Department of Agriculture (USDA), an executive department of the U.S. federal government charged with making and implementing government policies on agriculture, forestry, and food. USDA in the early 1990s to assess the impacts of alternative management practices on the resources of a watershed, particularly concerning water, sediment, nutrients, and pollution entering streams or water bodies within the watershed. SWAT is a hydrological model used to predict the effects of land management on water yield, sediment, pesticide loads, and agrochemicals (Gassman et al., 2014; Ikhwali et al., 2022).

The SWAT model has become one of the most widely used water quality and quantity and watershed assessment models worldwide and is used for a wide range of hydrological and environmental issues. The worldwide use of SWAT can be attributed to its ability to address water resources issues, which has been trained through many training

Table 3. Classification of density at Pasi Gusung Island

Sub-district/village	Population	Area (ha)	Population density (people/ha)	Category
Bontobarusu	1,642.00	1,245.68	1.32	Low population
Kahu-Kahu	2,055.00	608.59	3.38	Low population
Bontolebang	982.00	451.74	2.17	Low population

workshops and international conferences over the past decades. It includes extensive supporting documents and software, as well as open-source code that can be customized by model users for specific application needs (Gassman et al., 2014).

The SWAT model divides a watershed into several sub-watersheds to improve calculation efficiency. This approach is beneficial when areas within a watershed have different land uses and soil types, which uniquely affect hydrology. Each subwatershed has inputs grouped into categories such as climate, hydrologic response units (HRUs), ponds/wetlands, groundwater, primary channels, and subwatershed drainage. HRUs are the minor land units within a Subwatershed that have unique land cover, soil type, and management or a combination of all three (Hidayat, 2023).

This study used a variety of data sources, including climate projections, historical hydrological and meteorological data, as well as geographical data (Zhao et al., 2022), all of which are explained below:

- Aster digital elevation model (DEM) map data with 30 × 30 m (Rostami et al., 2022) obtained from Japan Space Systems (gdemdl.aster.jspacesystems.or.jp).
- The prepared climate data consisted of daily rainfall, daily maximum-minimum temperature, humidity, daily minimum and maximum temperature, sunshine duration, and daily average wind speed (Zhao et al., 2022). For 2015–2023, the climate data was obtained from https://power.larc.nasa.gov/data-access-viewer/
- Soil data (Zhao et al., 2022) was obtained from the land system data of the Regional Physical Planning Project or Transmigration (RePPProt) of the National Survey and Mapping Coordination Agency in 1987.
- Ministry of Environment and Forestry land cover map data 2023.
- Data analysis in this study was aimed at the QSWAT simulation process following the process below:

Subwatershed boundary delineation

Watershed delineation aims to produce watershed model data, as well as sub-watersheds and river networks. The threshold method is used in the watershed delineation process. The threshold amount determines the formation and number of significant river networks and tributaries. On the basis of the river network, the number of sub-watersheds formed in the watershed will be determined (Molina-Navarro et al., 2018). The stages carried out in the watershed delineation process consist of: DEM data input (add DEM grid), determination of the river network (stream definition), outlet determination (outlet and inlet definition), watershed outlet determination (watershed outlet selection and definition), and calculation of sub-watershed parameters (calculate subbasin parameters).

Establishment of HRU

The HRU is a hydrologic analysis unit based on specific soil characteristics, land use, and slope class. HRU analysis defines input data through overlaying land use maps, soil maps, and slope classes (Landuse/Soil/Slope definition). At this stage, an overlay was made between the results of DEM data, land use data, and soil data. HRU creation consists of slope intervals, land raster maps and soil raster maps in UTM (Universal Transverse Mercator) projection coordinate system format (Molina-Navarro et al., 2018).

Climate data processing

Climate data in QSWAT simulation consists of rainfall and temperature data at stations representing watershed areas and Weather Generator data in the form of solar radiation, wind speed, temperature, rainfall, and dew point. After inputting climate data, the running process was continued by utilizing the QSWAT Simulation menu. The climate data required is in the form of daily data on rainfall, maximum and minimum temperatures, solar radiation and wind speed. Each daily data for 10 years is processed in the WGN database (Tan et al., 2021) which requires 14 parameters, including:

- TMPMX average of the maximum temperature (°C),
- TMPMN, average of the minimum temperature (°C),
- TMPSTDMX standard deviation of daily maximum temperature (°C),
- TMPSTDMN standard deviation of daily minimum temperature (°C),
- PCPMM average rainfall (mm),
- PCPSTD standard deviation of daily rainfall (mm/day),
- PCPSKW skew coefficient for rainfall in one month,

- PR_W1 comparison of possible wet days – dry days in one month,
- PR_W2 comparison of possible wet days – wet days in one month,
- PCPD average number of rainy days in a month,
- RAINHHMX maximum 0.5 hour rainfall (mm),
- SOLARAV average daily solar irradiation in one month (MJ/m^2/day),
- DEWPT daily average dew point temperature in one month (°C),
- WINDAV daily average wind speed in one month (m/s),
- SWAT model run.

After the watershed delineation stage, HRU formation, and climate data processing, the last step is to run the model and simulate it. SWAT simulation is done after all input data is filled in completely. The SWAT run mode can be selected according to the time range to be simulated. Then, SWAT setup is carried out and SWAT is run. Saving the output data of simulation results is done by selecting read SWAT output.

SWAT analysis was carried out twice, namely for LULC 2023 and the prediction of LULC 2033. After obtaining the results of groundwater availability through SWAT analysis for 2023 and prediction of water availability in 2033, a comparison calculation of water availability with the total water demand for 1 year was carried out with the following formula:

$$\frac{water\ availability\ in\ the\ Pasi\ watershed}{the\ current\ population\ of\ Pasi\ Gusung\ Island \times \frac{60\ l}{\frac{person}{day}}} \quad (1)$$

RESULTS AND DISCUSSION

Results of cellular automata analysis with artificial neural network

In the CA analysis with ANN used is Landsat 8-9 OLI/TIRS C2 L2 image data (accessed on October 19, 2024) using bands 6,5,4 to see differences in land cover with false color combination, which is a technique that changes the original color of the image to show details that are usually not visible in natural colors. This technique is often used in satellite image analysis or remote sensing to observe vegetation, water, and land use. In determining land use classification, the supervised classification method is used by first selecting the land cover through the digitization process. The digitation process in remote sensing is a technique to convert information from analog images or raster maps into digital data in vector form that can be analyzed further.

Land cover prediction modeling using the Mollusce plugin in the QGIS application includes several stages, including:

Inputs

The input data is previously digitized land cover raster data, 2014 land cover as initial data and 2019 land cover as final data. The driving data is the 2023 population density data, which has been processed into a spatial format (.Shp form) and then converted into a raster map entered into the spatial variables column. Next, a geometry check was performed to evaluate the match between the driving factor raster data and the land cover data.

Evaluating correlations

In this stage, there are three types of correlation evaluation: Pearson's correlation, Cramer's coefficient, and joint information uncertainty. This research used Pearson's correlation method to determine the relationship between driving factors.

Cellular automata simulation

This stage is where the land cover prediction modeling process is performed. At the cellular automata simulation stage in MOLUSCE, multiples apply. The initial year is 2014 and the final year is 2019, then the prediction results are simulation data in 2023. To predict 2033, 3 iterations are needed.

Validation

This validation uses the image of the 2023 classification results as the referenced map and the 2023 simulation results as the simulated map. From the simulation results, the kappa (overall) value is 0.75, kappa (histo) is 0.79 and kappa (loc) is 0.95, where the kappa value obtained is included in the "excellent" category.

Land cover projection 2033

The 2033 land cover prediction results in 6 land classifications (Figure 2) including

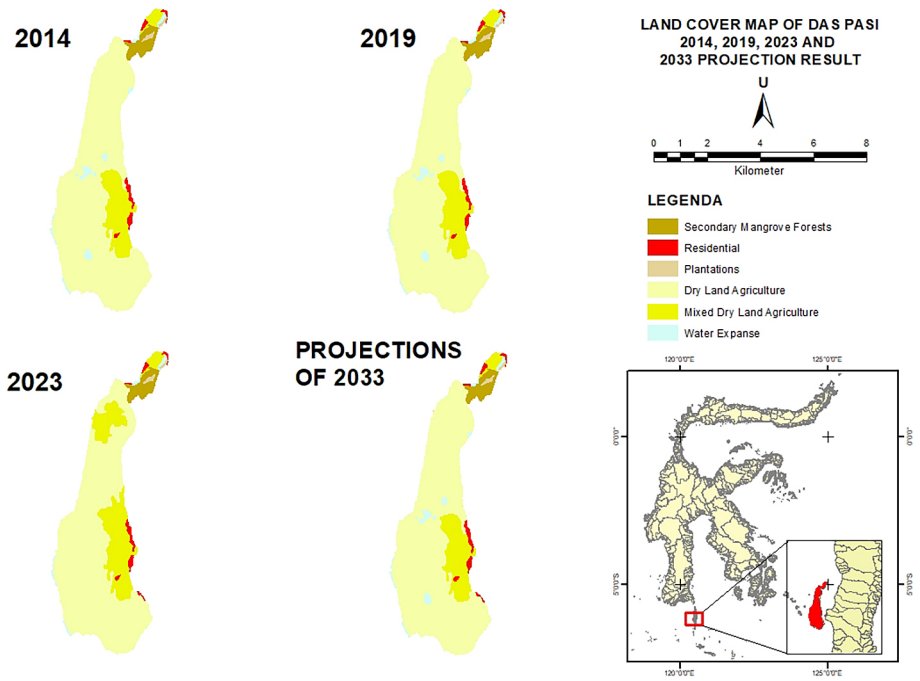

Figure 2. Land cover with 6 classifications on Pasi Gusung Island in 2014, 2019, 2023, and projected in 2033

secondary mangrove forests, residential, plantations, dry land agriculture, mixed dry land agriculture and water expanse. The following distribution of the existing land cover area in 2023 and the 2033 prediction results can be seen in the Tables 4 and 5, as well as the land use change and land cover maps above show spatial distribution of each category over 2014, 2019, 2023, and projected 2033. The most significant changes are in mixed dryland agriculture areas, which tend to decrease and convert to dryland agriculture and water bodies. Meanwhile, settlement areas remain fixed, with a slight expansion inland. The increase in dryland farming areas reflects the pressure on natural resources, such as deforestation for agricultural expansion. A decrease in mixed dryland farming could be due to changes in farming practices or conversion to other uses, such as residential areas or water bodies.

Result of SWAT analysis

Sub-watershed delineation

Delineation of sub-watershed boundaries is the initial stage carried out for SWAT analysis using 30-meter resolution DEMNAS data, as shown below in Figure 4. Slope class maps were automatically generated from DEM maps using the multiple slope method to produce five slope classes with slope classes of 0–8% (flat), 8–15% (gentle), 15–25% (moderately steep), 25–45% (steep), > 45% (very steep).

Sub-watershed delineation in the SWAT model is done automatically using DEM data, which results in watershed boundaries, sub-watershed

Table 4. Land cover change

Clasifications	Area (ha)		Selisih		Note
	Existing land cover (2023)	Land cover predictions (2033)	ha	%	
Secondary mangrove forestS	75.75	75.13	0.61	0.81	Reduce
Residential	39.16	40.22	-1.07	2.66	Increase
PlantationS	11.68	11.71	-0.03	0.26	Increase
Dry land agriculture	1680.53	1822.46	-141.92	7.79	Increase
Mixed dry land agriculture	460.20	285.07	175.14	38.06	Reduce
Water expanse	21.10	53.83	-32.73	60.80	Increase
Total	2288.42	2288.42			

Table 5. Comparison of land cover change

	Land cover classifications	2033 (ha)						Total
		Secondary mangrove forests	Residential	Plantations	Dry land agriculture	Mixed dry land agriculture	Water Expanse	
2023 (ha)	Secondary mangrove forests	74.76	0.07	0.22	0.35	0.30	0.05	75.75
	Residential		39.16					39.16
	Plantations		0.14	11.37			0.17	11.68
	Dry land agriculture		0.01		1645.43	1.34	33.76	1680.53
	Mixed dry land agriculture		0.78		176.12	283.07	0.24	460.20
	Water expanse	0.38	0.07	0.12	0.56	0.35	19.62	21.10
Total		75.13	40.22	11.71	1822.46	285.07	53.83	2288.42

Note: unchanged.

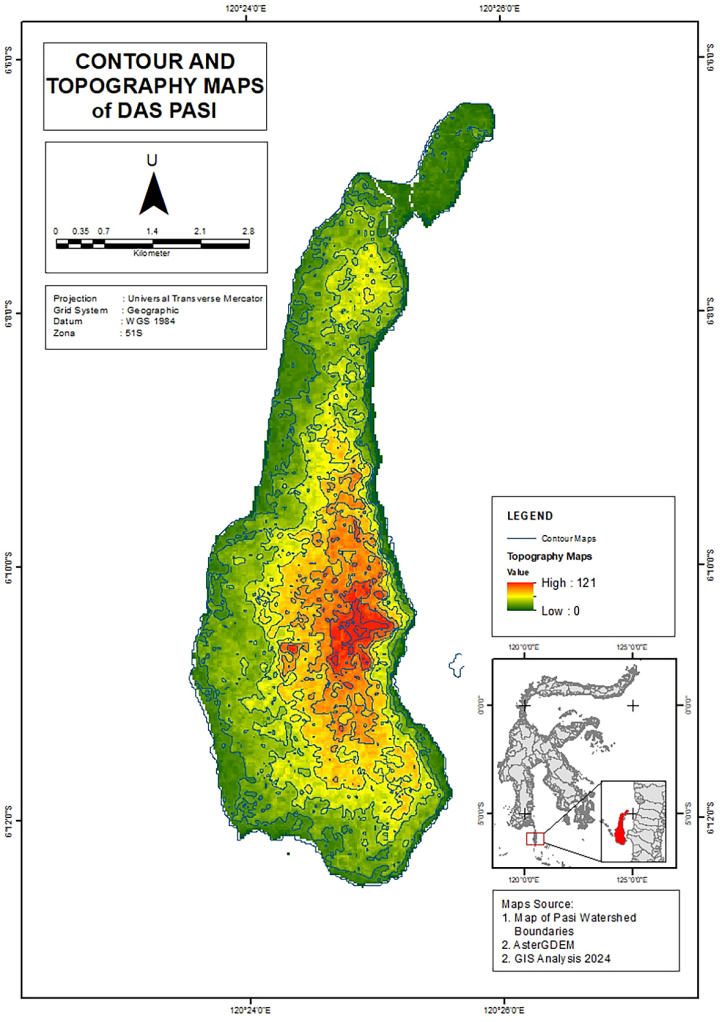

Figure 3. Contour and topography maps of PASI Island

boundaries, and river networks (Figure 3). This watershed delineation uses a 10 ha threshold to cover the entire river network in the Pasi watershed. Through delineation, watershed boundaries were formed with a total area of 1,705.07 ha and 90 sub-watersheds. The sub-watershed delineation can be seen in Table 6 and Figure 5. On the basis of the results of the delineation of PASI sub-watershed boundaries, the sub-watershed that has the most significant area is sub-basin 44 with an

Table 6. Sub-watershed division based on delineation results

Sub Watershed	Area	
	(ha)	(%)
1	2.49	0.15
2	11.87	0.70
3	3.54	0.21
4	15.22	0.89
5	20.10	1.18
6	3.73	0.22
7	4.98	0.29
8	23.55	1.38
9	17.61	1.03
10	0.96	0.06
11	9.67	0.57
12	22.40	1.31
13	23.83	1.40
14	4.79	0.28
15	19.14	1.12
16	31.97	1.87
17	3.35	0.20
18	40.77	2.39
19	4.50	0.26
20	0.48	0.03
21	2.87	0.17
22	26.32	1.54
23	6.41	0.38
24	29.48	1.73
25	11.96	0.70
26	10.82	0.63
27	10.53	0.62
28	18.47	1.08
29	36.37	2.13
30	27.28	1.60
31	15.98	0.94
32	10.82	0.63
33	52.83	3.10
34	12.06	0.71
35	20.87	1.22
36	13.50	0.79
37	27.85	1.63
38	28.81	1.69
39	46.23	2.71
40	15.41	0.90
41	38.19	2.24
42	29.19	1.71
43	13.40	0.79
44	80.50	4.72
45	22.49	1.32
46	20.67	1.21
47	25.84	1.52
48	20.20	1.18
49	14.45	0.85
50	18.95	1.11
51	19.05	1.12
52	13.11	0.77
53	12.44	0.73
54	29.86	1.75
55	24.22	1.42
56	36.47	2.14
57	11.29	0.66
58	16.18	0.95
59	19.81	1.16
60	23.74	1.39
61	11.20	0.66
62	11.77	0.69
63	13.21	0.77
64	22.68	1.33
65	24.31	1.43
66	13.30	0.78
67	20.67	1.21
68	12.06	0.71
69	10.91	0.64
70	28.43	1.67
71	13.21	0.77
72	28.81	1.69
73	14.64	0.86
74	11.20	0.66
75	10.72	0.63
76	20.96	1.23
77	40.39	2.37
78	15.89	0.93
79	13.78	0.81
80	20.10	1.18
81	12.54	0.74
82	14.07	0.83
83	45.85	2.69
84	16.46	0.97
85	10.05	0.59
86	16.94	0.99
87	14.26	0.84
88	10.62	0.62
89	12.25	0.72
90	13.88	0.81
Total	1,705.07	100.00

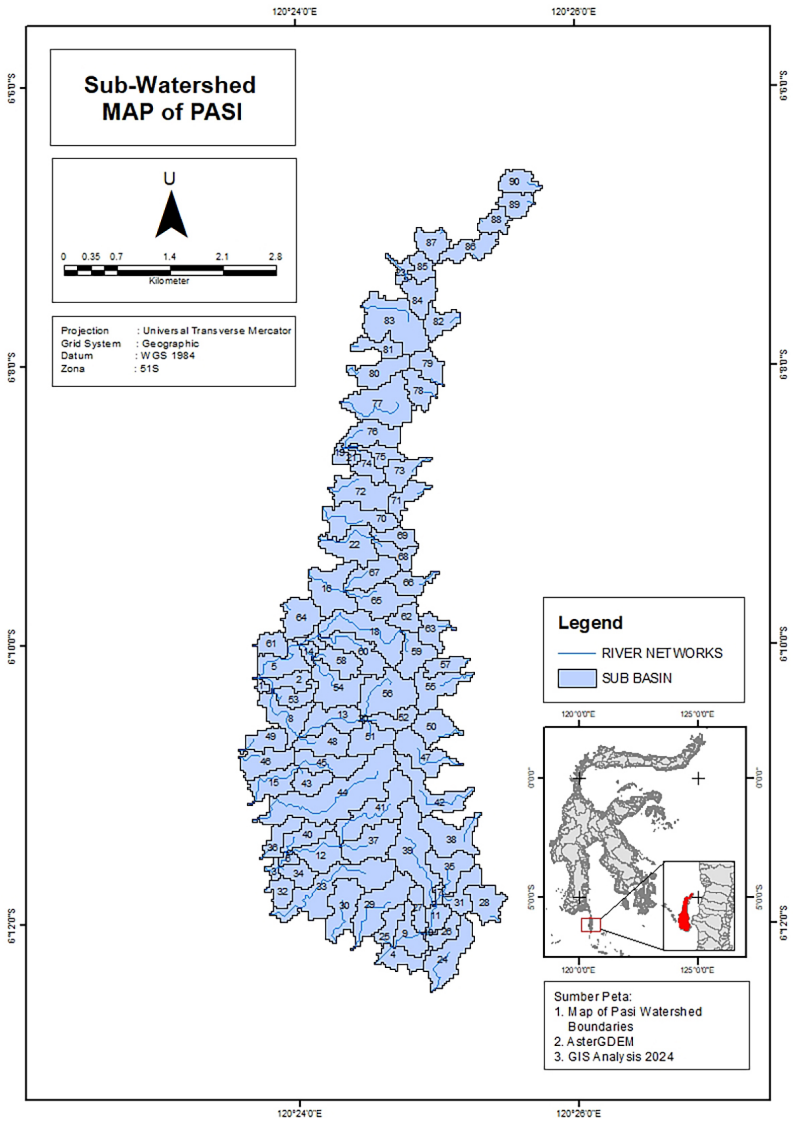

Figure 4. Sub-watershed maps

area of 80.50 ha (4.72%) and the smallest sub-watershed is sub-basin 20 with an area of 0.48 ha (0.03%).

Establishment of HRUs

The hydrology response unit (HRU) is the smallest unit of analysis in the SWAT model used for hydrological calculations. HRU formation is done through an overlay process between the land cover map, soil type map, and slope class. HRU analysis requires input data in the form of spatial and numerical data. Spatial data includes land cover maps, soil type maps, and slope classes, while numerical data includes soil characteristics, including its physical and chemical properties. The land cover map used was the 2023 map and the 2033 land cover projection results for the Pasi watershed. Soil numerical data were input into the SWAT database through the Edit SWAT Input mode. HRUs were formed based on the overlay results of the three types of input data.

Climate data processing

Climate data was downloaded through the old site https://power.larc.nasa.gov/data-access-viewer/ (accessed on October 26th, 2024) and sourced from the NASA/POWERCERES/MERRA-2 (Modern-era retrospective analysis for research and applications, version 2) satellite. The number of rainfall stations used consists of 4 stations. The climate data used in this study is in the form of daily climate data for the last 10 years

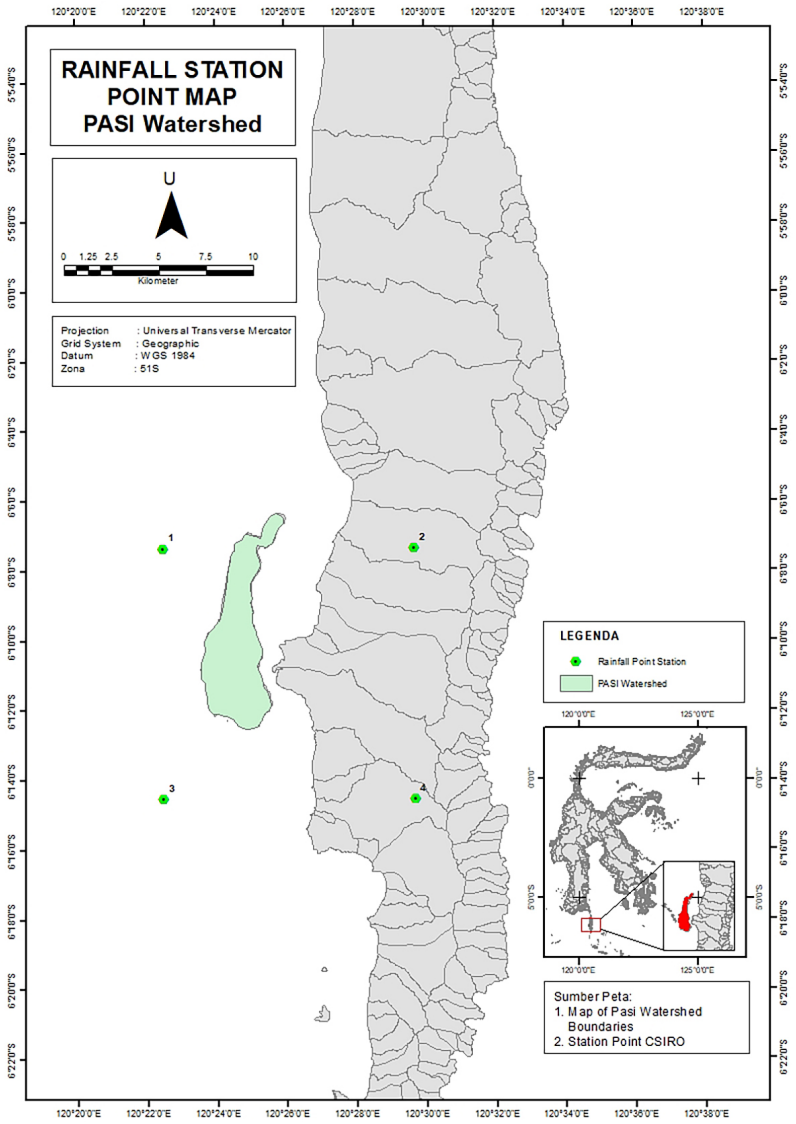

Figure 5. Rainfall station point map of Pasi watershed

(2014–2023). The climate data contains rainfall data (PRECTOTCORR), maximum temperature (T2M_MAX), minimum temperature (T2M_MIN), relative humidity (RH2M), shortwave radiation (TOA_SW_DWN), and wind speed (WS2M). The station point of climate data maps can be seen in Figure 5.

SWAT analysis result

Following all the processes, the results of the analysis of groundwater discharge in the Pasi watershed can be seen in Tables 7 and 8 for groundwater availability from 2014 to 2023, whereas the prediction of groundwater availability for the next 10 years, namely 2024–2033 in Table 9 and 10, which is calculated from the predicted population for the next 10 years using the following exponential growth formula.

$$r = \frac{(Pn - P0)}{P0 \times n} \quad (2)$$

On the basis of the SWAT analysis results in Tables 7 and 8, the annual water discharge from 2014 to 2023 fluctuates significantly in water availability, with a peak in 2021 of 465,125.10 m³/year or 465,125.100 liters/year and the lowest value in 2023 of 256,414.56 m³/year or 256,414.560 liters/year. However, this water availability is accompanied by population growth, which continues to grow from 4,493 people in 2014 to 4,679 people in 2023. As the population increases, the annual water demand increases from 98,396.700 liters in 2014 to 102,470.100 liters in 2023. The table shows that water demand is much greater

Table 7. SWAT analysis results for monthly water discharge for 2014–2023

Year	Debit (cm^3/s)												Total (cm^3/s)
	Month												
	1	2	3	4	5	6	7	8	9	10	11	12	
2014	4.11	1.91	1.86	1.84	0.34	0.56	0.16	0.02	0.00	0.00	0.10	2.16	13.06
2015	2.36	1.81	1.26	1.03	0.13	0.22	0.02	0.00	0.00	0.00	0.03	2.00	8.87
2016	1.01	1.46	0.62	0.29	0.17	0.32	0.29	0.04	0.09	0.67	0.29	1.15	6.40
2017	1.87	1.41	0.79	0.60	0.21	1.20	0.33	0.16	0.07	0.08	0.77	2.31	9.81
2018	2.85	2.33	1.89	0.58	0.15	0.32	0.67	0.06	0.01	0.00	0.29	1.24	10.38
2019	2.35	0.85	1.33	1.14	0.16	0.16	0.03	0.00	0.00	0.00	0.01	0.35	6.38
2020	1.08	1.47	1.87	0.32	0.96	0.27	0.14	0.30	0.06	0.09	0.51	2.95	10.03
2021	3.85	1.68	2.21	1.16	0.31	0.27	0.24	0.30	0.35	0.17	1.40	2.81	14.75
2022	2.05	2.64	0.92	0.30	1.25	1.00	0.33	0.25	0.18	1.02	1.19	2.83	13.96
2023	2.00	3.44	1.07	0.66	0.14	0.19	0.25	0.02	0.01	0.00	0.12	0.24	8.13

Table 8. SWAT analysis results for monthly water discharge for 2014–2023 (continued)

Year	cm^3/s	cm^3/year	L/year	Total population	Population demand per year	Difference between availability and demand
2014	0.0000131	413.12	413,124.54	4.493	98,396,700	-97,983,575.46
2015	0.0000089	279.57	279,574.51	4.555	99,754,500	-99,474,925.49
2016	0.0000064	202.36	202,361.01	4.543	99,491,700	-99,289,338.99
2017	0.0000098	309.34	309,344.40	4.587	100,455,300	-100,145,955.60
2018	0.0000104	327.26	327,255.30	4.601	100,761,900	-100,434,644.70
2019	0.0000064	201.10	201,097.54	4.632	101,440,800	-101,239,702.46
2020	0.0000100	317.19	317,185.22	4.682	102,535,800	-102,218,614.78
2021	0.0000147	465.13	465,125.10	4.682	102,535,800	-102,070,674.90
2022	0.0000140	440.37	440,366.72	4.680	102,492,000	-102,051,633.28
2023	0.0000081	256.41	256,414.56	4.679	102,470,100	-102,213,685.44

Table 9. SWAT analysis results for monthly water discharge for 2024–2033

Year	Debit (cm^3/s)												Total (cm^3/s)
	Month												
	1	2	3	4	5	6	7	8	9	10	11	12	
2024	1.64	0.58	0.51	0.74	0.05	0.02	0.04	0.00	0.01	0.34	0.53	0.95	5.41
2025	2.37	3.53	1.89	1.18	0.24	0.44	0.10	0.01	0.00	0.00	0.16	1.85	11.77
2026	2.93	2.56	0.91	0.50	0.15	0.28	0.04	0.01	0.01	0.01	0.43	4.40	12.22
2027	2.71	4.85	1.53	0.57	0.19	0.10	0.05	0.01	0.01	0.10	1.11	2.29	13.51
2028	5.09	4.34	1.28	0.55	0.18	0.06	0.08	0.01	0.04	0.01	0.35	1.36	13.34
2029	3.31	1.83	1.03	0.55	0.94	0.80	0.61	0.32	1.38	0.68	0.68	3.63	15.76
2030	3.15	2.97	2.48	1.35	0.44	0.14	0.03	0.01	0.02	0.07	0.64	4.51	15.79
2031	2.20	2.12	3.95	0.48	0.39	0.13	0.26	0.02	0.01	0.02	0.10	1.53	11.20
2032	4.88	2.27	1.93	1.92	0.48	1.73	0.61	0.17	0.02	0.05	0.70	3.75	18.51
2033	4.79	2.27	1.98	1.83	0.38	0.65	0.20	0.03	0.01	0.00	0.10	2.18	14.42

than water availability yearly. This difference expressed in the column "Difference between Availability and Demand" is always negative, indicating an ongoing water deficit. The most significant deficit occurred in 2017 at -100,145,955.60 liters, while the smallest deficit occurred in 2021 at -102,007,674.90 liters, marking a slight increase in water availability in that year.

Table 10. SWAT analysis results for monthly water discharge for 2024–2033 (continued)

Year	cm^3/s	cm^3/year	L/year	Total population	Population demand per year	Difference between availability and demand
2024	0.000005406	170.96	170,964.74	4,700	102,931,215	-102,760,250.71
2025	0.000011767	371.09	371,094.56	4,721	103,393,185	-103,022,090.44
2026	0.000012224	386.56	386,558.42	4,742	103,855,155	-103,468,596.13
2027	0.000013514	426.16	426,162.55	4,763	104,317,124	-103,890,961.55
2028	0.000013342	420.76	420,756.28	4,784	104,779,094	-104,358,337.37
2029	0.000015762	497.07	497,072.90	4,806	105,241,063	-104,743,990.30
2030	0.000015794	499.46	499,456.74	4,828	105,725,031	-105,225,574.56
2031	0.000011204	353.32	353,318.45	4,850	106,208,999	-105,855,680.95
2032	0.000018510	583.73	583,731.86	4,872	106,692,968	-106,109,235.64
2033	0.000014423	454.85	454,852.41	4,894	107,176,936	-106,722,083.19

Tables 9 and 10 show the results of SWAT analysis on the results of land cover projections for 2024-2033. The most minor discharge occurred in 2024 with 170,964.74 m^3/year (170,964.740 liters/year), while the most significant discharge was recorded in 2032 with 583,731.86 m^3/year (583,731,860 liters/year). Overall, there will be an increasing trend in water availability from 2024 to 2033, although this value will still be relatively small compared to demand. However, this is also in line with the projected population growth that continues to gradually increase from 4.700 people in 2024 to 4.894 people in 2033. Along with the increase in population, water demand continues to grow yearly. In 2024, water demand was 102,931.215 liters; in 2033, it increased to 107,176.936 liters. Water demand far exceeds water availability yearly, resulting in a persistent deficit. The smallest deficit occurs in 2024 at -102,760,250.71 liters, while the most significant deficit is projected to happen in 2033 at -106,722,083.19 liters.

CONCLUSIONS

This study showed a close relationship between land use and land cover changes and fluctuations in groundwater availability in the Pasi watershed. Analysis of land cover from 2014 to 2023 and projections to 2033 show patterns of change that affect the area's hydrology, including groundwater discharge and the balance between water availability and demand. Land cover change dominated by the expansion of dryland agriculture and the reduction of secondary mangrove forests contributes to the deficit in groundwater availability. Continued population growth pressures already limited water resources, creating a growing annual water deficit. This research provides strategic insights for developing sustainable water supply systems in response to projected land use change.

This research needs to be further explored and viewed from several additional aspects, such as socio-economic aspects, spatial distribution of land cover on water discharge and other factors related to hydrological processes in the Pasi watershed area. These shortcomings open opportunities for more comprehensive in-depth research with a multidisciplinary approach to face future water resources management challenges.

Acknowledgements

Funding support for this research and publication of this article was supported by the Center for Planner Development, Education, and Training (Pusbindiklatren) of Bappenas. Also commended is the Hasanuddin University Regional Development Planning Study Program, which approved the research. This research is part of a thesis submitted as a partial fulfillment of the requirements.

REFERENCES

1. Abbas, Z., Yang, G., Zhong, Y., & Zhao, Y. (2021). Spatiotemporal change analysis and future scenario of lulc using the CA-ANN approach: A case study of the greater bay area, China. *Land*, *10*(6). https://doi.org/10.3390/land10060584
2. Degerli, B., & Çetin, M. (2022). Using the remote sensing method to simulate the land change in the year 2030. *Turkish Journal of Agriculture - Food Science and Technology*, *10*(12), 2453–2466. https://

doi.org/10.24925/turjaf.v10i12.2453-2466.5555

3. Diansyukma, A. (2021). Analysis of clean water supply for remote area: Study case at Sepatin village, Kutai Kartanegara Regency. *IOP Conference Series: Earth and Environmental Science*, *739*(1). https://doi.org/10.1088/1755-1315/739/1/012014
4. Dibs, H., Ali, A. H., Al-Ansari, N., & Abed, S. A. (2023). Fusion Landsat-8 Thermal TIRS and OLI Datasets for superior monitoring and change detection using remote sensing. *Emerging Science Journal*, *7*(2), 428–444. https://doi.org/10.28991/ESJ-2023-07-02-09
5. Falconer, R. A. (2022). Water security: Why we need global solutions. *Engineering*, *16*, 13–15. https://doi.org/10.1016/j.eng.2021.10.009
6. Gassman, P. W., Sadeghi, A. M., & Srinivasan, R. (2014). Applications of the SWAT model special section: Overview and insights. *Journal of Environmental Quality*, *43*(1), 1–8. https://doi.org/10.2134/jeq2013.11.0466
7. Government of Selayar Islands Regency. (2023). *Strategic Environmental Assessment Report for the Detailed Spatial Plan of Pasi Gusung Island*.
8. Hidayat, Y. (2023). *Step by Step Model SWAT*. Department of Soil Science and Land Resources, IPB University.
9. Hotloś, H. (2008). Quantity and availability of freshwater resources: The world - Europe - Poland. *Environment Protection Engineering*, *34*(2), 67–77.
10. Ikhwali, M. F., Rau, M. I., Nur, S., Ferijal, T., Prayogo, W., & Saputra, S. F. D. (2022). Application of soil and water assessment tool in Indonesia – A review and challenges. *Desalination and Water Treatment*, *277*, 105–119. https://doi.org/10.5004/dwt.2022.29018
11. Indhanu, N., Chalermyanont, T., & Chub-Uppakarn, T. (2025). Spatial assessment of land use and land cover change impacts on groundwater recharge and groundwater level: A case study of the Hat Yai basin. *Journal of Hydrology: Regional Studies*, *57*(April 2024), 102097. https://doi.org/10.1016/j.ejrh.2024.102097
12. Jamal, S., & Ahmad, W. S. (2020). Assessing land use land cover dynamics of wetland ecosystems using Landsat satellite data. *SN Applied Sciences*, *2*(11), 1–24. https://doi.org/10.1007/s42452-020-03685-z
13. Kim, Y., & Newman, G. (2020). *in Urban Land Change Models*. 1–22.
14. Liu, Z., Rong, L., & Wei, W. (2023). Impacts of land use/cover change on water balance by using the SWAT model in a typical loess hilly watershed of China. *Geography and Sustainability*, *4*(1), 19–28. https://doi.org/10.1016/j.geosus.2022.11.006
15. Martin, N. (2021). Risk assessment of future climate and land use/land cover change impacts on water resources. *Hydrology*, *8*(1), 1–23. https://doi.org/10.3390/hydrology8010038
16. Mishra, B. K., Kumar, P., Saraswat, C., Chakraborty, S., & Gautam, A. (2021). Water Security in a Changing Environment : Concept,. *Water*, *13*(4), 490.
17. Molina-Navarro, E., Nielsen, A., & Trolle, D. (2018). A QGIS plugin to tailor SWAT watershed delineations to lake and reservoir waterbodies. *Environmental Modelling and Software*, *108*, 67–71. https://doi.org/10.1016/j.envsoft.2018.07.003
18. Nedd, R., Light, K., Owens, M., James, N., Johnson, E., & Anandhi, A. (2021). Knowledge gaps on a global landscape. *Land*, *10*(2020), 1–30.
19. Pan, R., Martinez, A., Brito, T., & Seidel, E. (2018). Processes of soil infiltration and water retention and strategies to increase their capacity. *Journal of Experimental Agriculture International*, *20*(2), 1–14. https://doi.org/10.9734/jeai/2018/39132
20. Rostami, A., Raeini-Sarjaz, M., Chabokpour, J., Azamathulla, H. M., & Kumar, S. (2022). Determination of rainfed wheat agriculture potential through assimilation of remote sensing data with SWAT model case study: ZarrinehRoud Basin, Iran. *Water Supply*, *22*(5), 5331–5334. https://doi.org/10.2166/ws.2022.160
21. Setiawan, O., & Nandini, R. (2022). Integration of LULC change/prediction and hydrological modeler for assessment of the effect of LULC Change on peak discharge in Sari Watershed, Sumbawa Island, Indonesia. *IOP Conference Series: Earth and Environmental Science*, *1109*(1). https://doi.org/10.1088/1755-1315/1109/1/012070
22. Sulamo, M. A., Kassa, A. K., & Roba, N. T. (2021). Evaluation of the impacts of land use/cover changes on water balance of bilate watershed, rift valley basin, Ethiopia. *Water Practice and Technology*, *16*(4), 1108–1127. https://doi.org/10.2166/wpt.2021.063
23. Tan, M. L., Gassman, P. W., Liang, J., & Haywood, J. M. (2021). A review of alternative climate products for SWAT modelling: Sources, assessment and future directions. *Science of the Total Environment*, *795*, 148915. https://doi.org/10.1016/j.scitotenv.2021.148915
24. Tong, X., & Feng, Y. (2020). A review of assessment methods for cellular automata models of land-use change and urban growth. *International Journal of Geographical Information Science*, *34*(5), 866–898. https://doi.org/10.1080/13658816.2019.1684499
25. Zhao, H., Li, H., Xuan, Y., Li, C., & Ni, H. (2022). Improvement of the SWAT model for Snowmelt runoff simulation in seasonal snowmelt area using remote sensing data. *Remote Sensing*, *14*(22). https://doi.org/10.3390/rs14225823